Correlation functions in the quadrupolar glass phase of solid hydrogen

N. S. Sullivan
Department of Physics, University of Florida, Gainesville, Florida 32611

M. Devoret*
Department of Physics, University of California, Berkeley, California 94720

D. Estève
Service de Physique du Solide et de Résonance Magnétique, Centre d'Etudes Nucléaires de Saclay, F-91191 Gif-sur-Yvette, France

(Received 25 May 1984)

A precise description of the molecular order parameters and their correlation functions that determine the NMR line shapes, damping of spin echoes, and the longitudinal nuclear relaxation in solid ortho-para hydrogen mixtures is given and the effects of fluctuations of the order parameters on the NMR measurements are discussed. This formalism is used to make precise definitions of terms such as "freezing," "dynamic gel," "glass formation," etc., that have been used in the literature to describe the NMR results. An operational definition of a "quadrupolar glass" is given in terms of the correlation functions and the different NMR techniques are analyzed to show what properties of the correlation functions can be deduced in each case. The time scale of the variations of the correlation functions probed by the different experiments is discussed in detail.

I. INTRODUCTION

There has been considerable experimental effort by several groups[1–31] in recent years to understand the orientational ordering of a random distribution of quadrupole-bearing molecules (such as ortho hydrogen) located at fixed sites in a matrix [the lattice is hcp for concentrations $x<55$ at. % (Ref. 28)] of spherical but otherwise "equivalent" molecules (parahydrogen species for solid H_2 mixtures). These studies have been stimulated by the realization[6] that a random distribution of electric quadrupoles represents a particularly striking example of the combined effects of frustration and disorder which play a dominant role in the local ordering observed in spin glasses (*Cu*Mn, *Au*Fe, alloys, etc.)[32–34] and in related systems [orientational glasses such as $(KCN)_x(KBr)_{1-x}$ mixtures,[35–37] electric dipolar glasses $KTaO_3$:Li,[38] etc.].

For axial quadrupoles the lowest-energy configuration of an isolated pair is a "tee" configuration with the molecular axes mutually perpendicular, but it is impossible to arrange all molecular axes mutually perpendicular on any three-dimensional (3D) lattice. This frustration[6] results in a topological incompatibility between the orientational correlations in the ground state of small clusters of quadrupoles (pairs, triplets, etc.) and those of the ground-state configurations of the infinite system (there may be several almost-degenerate low-lying states in a dilute system[38]). For high quadrupole concentrations this leads to a first-order phase transition to the well-known Pa_3 configuration[39] which represents a compromise between the minimization of the different intermolecular interaction energies and the establishment of long-range orientational order. For concentrations below approximately 55 at. %, no simple long-range order has been observed experimentally (for temperatures down to approximately 50 mK), and it has been suggested[6,40] that for these concentrations, solid ortho-para hydrogen mixtures (and para-ortho deuterium mixtures) form a quadrupolar glass in which the local orientational-order parameters vary from site to site without any long-range spatial correlation, and fluctuations (if any) of these parameters occur for only very long time scales ($t \gg 10^{-5}$ sec). Following this speculation, many NMR experiments[14–21] have been reported, describing the "freezing" (Refs. 6–9, 14, and 19) or the apparent absence (Refs. 10, 11, 18, 20, and 21) of "freezing" of the molecular orientations in solid H_2 (and solid D_2) mixtures, and the evolution of the molecular dynamics upon cooling. In order to clearly understand how different experimental techniques probe the orientational degrees of freedom and their time dependence, it is important that an unambiguous formulation be presented and precise definitions be given for various terms and notions, such as the "freezing" of the orientations, "dynamic gel," and "glass formation," which have been used rather loosely in the literature. The purpose of this paper is to present such a formulation and provide a framework that will allow us to analyze the different results more carefully and thereby compare the various interpretations quantitatively. (Summaries of the results obtained and conclusions reached by various groups can be found and compared in Ref. 41.)

II. ORIENTATIONAL-ORDER PARAMETERS AND CORRELATION FUNCTIONS

The first step in our procedure will be to specify the orientational degrees of freedom of an individual molecule. (A comprehensive discussion of this can be found in Ref. 17.) For ortho-H_2 (and para-D_2) the orbital angular

momentum J is a good quantum number, and the degrees of freedom are those of a spin-1 particle. In the absence of interactions which break time-reversal symmetry, the dipole moments $\langle J_X \rangle$, $\langle J_Y \rangle$, and $\langle J_Z \rangle$ vanish and we need only consider the higher-order components of a second-rank tensor $\langle Q_{\alpha\beta} \rangle$ which are the expectation values of the operator

$$Q_{\alpha\beta}=\tfrac{1}{2}(J_\alpha J_\beta+J_\beta J_\alpha)-\tfrac{1}{3}J^2 . \tag{1}$$

α and β refer to an arbitrary set of Cartesian axes (X,Y,Z). Of the nine components $\langle Q_{\alpha\beta} \rangle$, only five are independent. If we choose three local axes (x,y,z) which coincide with the principal axes of the tensor $\langle Q_{\alpha\beta} \rangle$, $\langle Q_{xy} \rangle=\langle Q_{yz} \rangle=\langle Q_{zx} \rangle=0$, and only two intrinsic quadrupolar parameters remain. These are

$$\sigma=\tfrac{3}{2}\langle Q_{zz} \rangle=\langle (1-\tfrac{3}{2}J_z^2) \rangle \tag{2a}$$

and

$$\eta=\frac{\sqrt{3}}{2}\langle (Q_{xx}-Q_{yy}) \rangle=\frac{\sqrt{3}}{2}\langle (J_x^2-J_y^2) \rangle . \tag{2b}$$

[The normalization factors in Eqs. (2a) and (2b) are chosen so that (σ,η) transform orthonormally when the axes are rotated.] The three local principal axes (x,y,z) and the order parameters (σ,η) constitute the five variables needed to completely specify the orientational degrees of freedom (when the components $\langle J_x \rangle$, $\langle J_y \rangle$, and $\langle J_z \rangle$ of the angular momentum are quenched).

Instead of the Cartesian components, it is more convenient to introduce the irreducible tensorial operators Θ_{2m}, which are the operator equivalents of the spherical harmonics Y_{2m} in the manifold $J=1$. We write

$$\Theta_{20}=1-\tfrac{3}{2}J_Z^2,\quad \Theta_{2,\pm1}=\pm(\tfrac{3}{8})^{1/2}(J_\pm J_Z+J_Z J_\pm) , \tag{3}$$

and

$$\Theta_{2,\pm2}=(\tfrac{3}{8})^{1/2}(J_\pm)^2 .$$

In the principal-axes reference frame, $\langle \Theta_{2,\pm1} \rangle=0$ and $\langle \Theta_{2,\pm2} \rangle$ are real, and we have

$$\sigma=\langle \Theta_{20} \rangle \text{ and } \eta=\langle \Theta_{2,2}+\Theta_{2,-2} \rangle/\sqrt{2} . \tag{4}$$

If the molecule is in a pure state, there are only three possibilities, $\sigma=1$ with $\eta=0$, or $\sigma=-\frac{1}{2}$ with $\eta=\pm\sqrt{3}/2$. These states are physically equivalent, as can be seen by a simple permutation of the axes x,y,z. In order to reduce this redundancy, we adopt the convention that, from the possible permutations of the principal axes, we choose the labels of the axes such that $|\sigma| > |\eta| \geq 0$.

In general, the system need not be in a pure state, and a density-matrix description becomes necessary. We then describe the degrees of freedom of each molecule by a single-particle 3×3 matrix operator[6]

$$\rho=\tfrac{1}{3}\mathbb{1}_3+\tfrac{2}{3}\sum_{m=0,\pm1,\pm2}\langle \Theta_{2m} \rangle \Theta_{2m}^\dagger . \tag{5}$$

In the local principal-axes frame, this can be written as

$$\rho=\tfrac{1}{3}\mathbb{1}_3+\begin{bmatrix} -\frac{1}{3}\sigma & 0 & \frac{1}{\sqrt{3}}\eta \\ 0 & \frac{2}{3}\sigma & 0 \\ \frac{1}{\sqrt{3}}\eta & 0 & -\frac{1}{3}\sigma \end{bmatrix} \tag{6}$$

in the representation $|J,J_z\rangle$ with the rows (columns) corresponding to $J_z=1,0,-1$.

The allowed values of σ and η are determined by the condition that the eigenvalues λ of the unitary matrix ρ be positive definite, i.e., that $0<\lambda<1$. The eigensolutions are

$$\lambda_1=\tfrac{1}{3}(1+2\sigma) \tag{7a}$$

and

$$\lambda_{2,3}=\tfrac{1}{3}(1-\sigma)\pm\frac{1}{\sqrt{3}}\eta . \tag{7b}$$

The allowed values of σ and η are therefore constrained to $-\frac{1}{2}\leq\sigma\leq1$ and $|\eta| \leq 1\pm(1/\sqrt{3})\sigma$. This is the triangular region in the (σ,η) plane shown in Fig. 1. The vertices correspond to the pure states discussed earlier. As shown for the pure states, not all points in the "allowed" triangle of Fig. 1 are inequivalent. Following our convention that we choose the labels of the principal axes such that $|\sigma| \geq |\eta| \geq 0$, we find that we need only consider the hatched region in Fig. 1 bounded by the lines

$$\eta=\pm\frac{1}{\sqrt{3}}\sigma \text{ and } \eta=0 .$$

As an aid to understanding the nature of the order parameters we can consider an ellipsoid whose axes are the

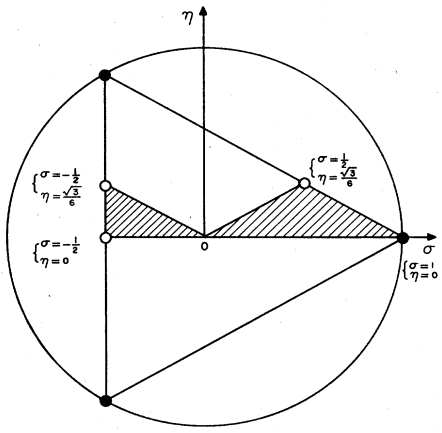

FIG. 1. Allowed values of the orientational order parameters $\sigma=\langle 1-\frac{3}{2}J_z^2 \rangle$ and $\eta=(\sqrt{3}/2)\langle J_x^2-J_y^2 \rangle$ of a spin-1 particle (without a dipolar moment) are restricted to the triangle bounded by the lines $\sigma=-\frac{1}{2}$ and $\eta=\pm(1/\sqrt{3})(1-\sigma)$ in (σ,η) space. x, y, and z are the principal axes for the quadrupole tensor $\langle \frac{1}{2}(J_\alpha J_\beta+J_\beta J_\alpha)-\frac{1}{3}J^2 \rangle$. Not all points inside the triangles are inequivalent, and by selecting the permutation of the principal axes (x,y,z) so that $\sigma\geq|\eta|\geq0$, we need only consider values inside the hatched region: $\eta\geq0$, $|\eta|<(1/\sqrt{3})\sigma$, and $-\frac{1}{2}<\sigma<-\sqrt{3}\eta$.

principal axes defined above, and plot the three eigenvalues $\lambda_1,\lambda_2,\lambda_3$ on these axes to determinate the boundaries of the ellipsoid. This ellipsoid can be regarded as representing a probability distribution for the molecular orientations with the probability that a molecule is oriented parallel to $\vec{R}$ being given by

$$\lambda_1\frac{R_x^2}{R^2}+\lambda_2\frac{R_y^2}{R^2}+\lambda_3^2\frac{R_z^2}{R^2}\ .$$

Figure 2 illustrates this description for (a) preferential alignment along an axis ($\sigma>0$), and (b) a molecule lying preferentially in a plane ($\sigma<0$). A measure of the overall departure from an isotropic distribution is given by the total quadrupolarization $q\equiv(\sigma^2+\eta^2)^{1/2}$.

With the above definitions of the irreducible operators Θ_{2m} and their expectation values which describe the orientational degrees of freedom of the $J=1$ molecules, we can construct an autocorrelation $G_i(t)$ for each molecule, given by

$$G_i(t)=\tfrac{1}{2}\sum_m\langle\Theta_{2m_i}(t)\Theta^\dagger_{2m_i}(0)+\Theta_{2m_i}(0)\Theta^\dagger_{2m_i}(t)\rangle_T\ , \tag{8}$$

where $\langle\ \rangle_T$ designates a statistical thermodynamic average. This autocorrelation function has the virtues of being a real scalar, independent of the choice of reference frame and the "nature" of the local quadrupolar order (i.e., axial or nonaxial). $G_i(t)$ has the following properties,

$$G_i(0)=\tfrac{5}{2},\quad G_i(\infty)=\sum_m|\langle\Theta_{2m_i}\rangle|^2=q_i^2\ , \tag{9}$$

where $q_i=(\sigma_i^2+\eta_i^2)^{1/2}$ is the magnitude of the total quadrupolarization of the ith molecule, and the parameters σ_i,η_i *must* be calculated in the local principal-axes reference frame. The behavior of $G_i(t)$ for a given time interval t is determined by the orientational motion of the molecule in that time interval. This molecular motion can be followed by using different NMR experiments. The general time dependence of the simple correlation function $G_i(t)$ is easy to understand in physical terms and can be constructed from the results of the different NMR studies. Instead of directly measuring the function $G_i(t)$, a given NMR experiment probes a particular combination of one or more of the correlation functions

$$\mathcal{G}_{m_i}(t)=\tfrac{1}{2}\langle\Theta_{2m_i}(t)\Theta^\dagger_{2m_i}(0)+\Theta_{2m_i}(0)\Theta^\dagger_{2m_i}(t)\rangle_T$$

[e.g., the spin-lattice relaxation rates are related to the Fourier transform of $\sum_{m=1,2}m^2\mathcal{G}_{m_i}(t)$]. Each type of experiment and the appropriate correlation functions must therefore be considered carefully for each case in order to be able to determine $G_i(t)$. These different methods are discussed in the following sections, and in Sec. VI we describe precisely how a quadrupolar glass should be defined in terms of the correlation functions.

It will be shown in Sec. VI that we are led naturally to define an "orientational glass" (or "glassy state") as one in which the molecular orientations become apparently "frozen" when studied over a time scale $t_{\rm scale}$, i.e, when

(i) $G(t)$ is flat for $t_{\rm micro}<t<t_{\rm scale}$

and

(ii) $G(t=t_{\rm scale})>q^2_{\rm eqm}$

where $q^2_{\rm eqm}$ is the statistical or equilibrium average of the quadrupolarization taken over *all* configurations and $t_{\rm micro}$ is a microscopic time scale associated with the molecular interactions (e.g., h/E_{QQ}). We can say that the molecular orientations appear to be "frozen" for the specified time scale if condition (i) is satisfied, and "glass formation" occurs if condition (ii) is also satisfied (i.e., if the system becomes nonergodic).

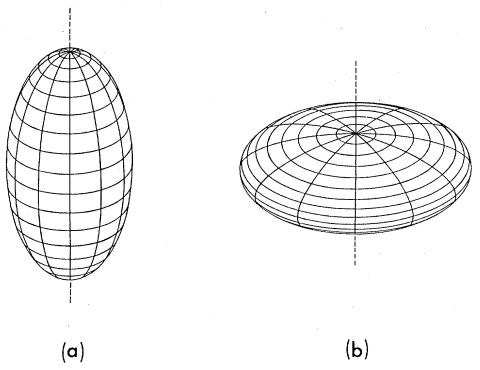

FIG. 2. Schematic representation of the probability distribution for the orientation of a molecule. The probability $P(\Omega)$ of finding a molecule oriented parallel to the vector $\vec{R}$ from the origin to the surface of the sphere is given by $P(\Omega)=(\lambda_1R_x^2+\lambda_2R_y^2+\lambda_3R_z^2)/R^2$. λ_n have the eigenvalues of the density matrix specifying the orientational degrees of freedom. Two cases are illustrated for (a) a molecule oriented preferentially along an axis $\sigma>0$, and (b) orientation preferentially in a plane, $\sigma<0$.

III. NMR LINE-SHAPE STUDIES

NMR techniques provide a particularly direct method for studying these order parameters since the perturbation of the nuclear Zeeman energy levels is determined by the secular component of the intramolecular nuclear dipole-dipole interaction $\mathcal{H}^{\rm sec}_{DD}$, which depends directly on the orientational state of the molecule. We have

$$\mathcal{H}^{\rm sec}_{DD}=\tfrac{2}{3}D(1-\tfrac{3}{2}I_Z^2)\langle1-\tfrac{3}{2}J_Z^2\rangle_T\ , \tag{10}$$

where

$$\frac{D}{2\pi}=\frac{3}{5}\frac{\gamma^2\hbar^2}{a^3}=173.06\ \text{kHz}\ ,$$

a being the internuclear separation. The quantization axis OZ is determined by the direction of externally applied magnetic field H_0. In order to relate this perturbation to the orientational state of the molecule we must transform to the local molecular reference triad determined by the principal axes (x,y,z) of the molecular quadrupole tensor. We then find[6]

$$\mathcal{H}^{\rm sec}_{DD}=\tfrac{2}{3}D(1-\tfrac{3}{2}I_Z^2)[\sigma P_2(\cos\theta)+\sqrt{3}\eta\sin^2\theta\cos2\phi]\ , \tag{11}$$

where θ and ϕ are the polar angles specifying the orientation of OZ in the local frame (x,y,z).

In order to determine the absorption line shape and NMR properties resulting from this perturbation, we need to know the time scale of any time dependence of the order parameters. If the parameters are static or if any fluctuations occur at frequencies less than D (i.e., quasistatic), then each molecule i contributes a doublet to the line shape with a frequency separation given by

$$\Delta\nu_i = \pm D[\sigma_i P_2(\cos\theta_i) + \sqrt{3}\eta_i \sin^2\theta_i \cos 2\phi_i] , \quad (12)$$

with respect to the Larmor frequency $\nu_L = \gamma\hbar H_0/2\pi$. For the case of axial symmetry ($\eta_i = 0$ at each site) and the same value of σ at each site ($\sigma = 1$ for the Pa_3 structure), one finds the familiar Pake-doublet line shape upon summing over all orientations for a powdered sample. (This consists of two cusps separated by $\delta\nu = D = 173.06$ kHz with shoulders extending to a separation of 346.1 kHz.) If there is a distribution of quasistatic order parameters $P(\sigma)$, then the line shape consists of a superposition of Pake doublets (assuming $\eta = 0$ at each site), and this approach has been used to infer distributions $P(\sigma)$ from the low-temperature line shapes for dilute mixtures with ortho concentrations of $x < 55$ at. %.[6,16,19] There is, however, no justification for the assumption of local axial symmetry in the dilute systems.

If the order parameters are not quasistatic, i.e., if fluctuations occur at a frequency comparable to D, then each doublet contribution to the line shape is motionally averaged; the satellites are reduced in intensity at the expense of a central motionally narrowed line which grows as the motional frequency increases beyond D. The analysis of the line shapes in terms of a superposition of Pake doublets would not be correct in this motional-narrowing regime and it is important to realize this in order to avoid confusing changes in $P(\sigma)$ with motional-narrowing effects. It is certainly erroneous to analyze the line shapes in terms of a distribution of static order parameters, and for the same sample and experimental conditions interpret pulsed NMR experiments (that explore the molecular dynamics) in terms of orientational fluctuations with frequencies ω_m comparable to $D \simeq 10^5$ Hz.

The motionally narrowed line shape can be calculated for one simple case,[42] namely a stationary Markov process involving a random hopping at rate Ω from one value of σ, $\sigma = \frac{1}{2}$, to the other, $\sigma = -\frac{1}{2}$. To lowest order the contributions to the line shapes from each molecule are found to be (a) for rapid transitions, $\Omega \gg DP_2(\theta_i)$, a motionally narrowed Lorentzian line with half-width at half-height

$$\Delta\nu_i = \frac{2}{3}\frac{\delta_i^2}{\Omega} , \quad (13)$$

where $\delta_i = DP_2(\cos\theta_i)$, and (b) for slow motion, $\Omega \ll DP_2(\theta_i)$, discrete lines at $\delta\nu_i = \pm\delta_i$ with half-widths Ω.

It should be noted that the spectral components δ_i depend on the geometrical factor $P_2(\cos\theta_i)$, and the motionally narrowed linewidth depends not only on the frequency Ω but also on the orientation $\cos\theta_i$ of the molecule's symmetry axis with respect to the local magnetic field. Molecules inclined at $\theta = \arcsin(1/\sqrt{3})$, i.e., those close to the "center" of the line shape ($\delta\nu$ small), would, in this model, lead to extremely narrow Lorentzian line shapes even for $\Omega \simeq D$. The NMR absorption spectrum would therefore include a narrow, peaked central component of the NMR line shapes at temperatures for which motion occurs in the frequency range $0.1D < \Omega < 10D$. One would expect this central component to broaden at low temperatures since the spectral density of the fluctuations in the interval $0.1D < \Omega < 10D$ would normally be expected to decrease rapidly with decreasing temperature.

Although a narrow central feature is actually seen in the NMR line shapes[3,5,6] for ortho hydrogen concentrations of $x < 55$ at. % and for temperatures $80 < T < 450$ mK, its persistence down to the lowest temperatures is not understood. A narrow component as also reported several years ago by Amstutz *et al.*[21,43] and others[1,3] for mixtures with high ortho concentrations, but the origin of this component was not discussed in those reports.

IV. NMR PULSE TECHNIQUES

One way of distinguishing between motional-narrowing effects on cw line shapes and changes in the distribution of the quasistatic order parameters is to study the damping of solid echoes formed by two 90° rf pulses, one of which rotates the spins by 90° about the x axis, and the other by 90° about the y axis at time τ after the first pulse. If we consider *only* the intramolecular nuclear dipole-dipole interactions, then the amplitude of the solid echo formed at $t = 2\tau$ is the sum of the following contributions from each molecule:

$$E_j(2\tau) = \mathrm{Tr}\exp\left[i\hbar^{-1}\int_\tau^{2\tau}\mathscr{H}_{DD_j}dt\right]R_y\left[\frac{\pi}{2}\right]\exp\left[i\hbar^{-1}\int_0^{\tau}\mathscr{H}_{DD_j}dt\right]I_{x_j}\times\cdots$$
$$\cdots\times\exp\left[-i\hbar^{-1}\int_0^{\tau}\mathscr{H}_{DD_j}dt\right]R_y^{\dagger}\left[\frac{\pi}{2}\right]\exp\left[-i\hbar^{-1}\int_\tau^{2\tau}\mathscr{H}_{DD_j}dt\right]I_{x_j} ,$$

where $\mathscr{H}_{DD_j}$ is the secular part of the spin-spin interaction between the two nuclei of molecule j,

$$\mathscr{H}_{DD_j}^{\mathrm{sec}} = \hbar\tfrac{2}{3}D(1-\tfrac{3}{2}I_Z^2)\sigma_j P_2(\cos\theta_j) + \sqrt{3}\eta_j\sin^2\theta_j\cos 2\phi_j .$$

Assuming, for simplicity, that we have axial symmetry ($\eta_j = 0$), then

$$E_j(t=2\tau)=\exp\left[iD\left[\int_\tau^{2\tau} dt\,\sigma_j(t)P_2[\cos\theta_j(t)]-\int_0^\tau dt\,\sigma_j(t)P_2[\cos\theta_j(t)]\right]\right], \tag{14}$$

where we have allowed for time dependence in both the order parameter σ_j and the orientation θ_j of the symmetry axis.

Obviously, if the parameters σ and P_2 vary very slowly in the two time intervals of length τ, i.e., if $D\tau \gg 1$, then $E_j(2\tau)=1$ and there is no motional damping. In the other limit of very fast motion, both of the above time averages $\int_0^\tau dt$ and $\int_\tau^{2\tau} dt$ become negligible, $|D\int \sigma P_2(\theta)| \ll 1$, and also in this limit, $E_j(2\tau)=1$ and there is no motional damping. (The inclusion of magnetic interactions between different molecules would, of course, lead to an attenuation of the echoes, but this is distinct from the motional effects we are considering here.)

Motional damping becomes effective when the time dependence of σ_j and θ_j in the two time intervals $0<t<\tau$ and $\tau<t<2\tau$ is such that the time averages $D\int_\tau^{2\tau} dt\,\sigma P_2(t)$ and $D\int_0^\tau dt\sigma P_2(t)$ interfere destructively. The echo will then be damped by the motion. This occurs, in general, for motional frequencies in the range $0.1D<\omega_m<10D$. As an example we can consider θ as fixed, while allowing σ to fluctuate. In this case, the averages over the time dependence may be written as

$$\exp\left[-\tfrac{3}{2}iDP_2(\theta_j)\left[\int_\tau^{2\tau}-\int_0^\tau\right]\sigma_j(t)dt\right]$$

for the jth molecule. We have

$$\phi_j=\tfrac{3}{2}DP_2(\theta_j)\left[\left[\int_0^{2\tau}-\int_0^\tau\right]\sigma_j(t)dt\right],$$

which represents the total phase shift ϕ_j for the jth molecule induced by the fluctuations in σ_j. If the motion is largely uncorrelated and fast, so that for a given θ_j the phase shift accumulated after time τ has a Gaussian distribution function, then the average

$$\begin{aligned}\langle\exp(-i\phi)\rangle_{\rm av}&=\exp(-\tfrac{1}{2}\langle\phi^2\rangle)\\&=\exp\left[-\tfrac{1}{2}[DP_2(\cos\theta_j)]^2\left\langle\int_\tau^{2\tau}dt_1\int_0^\tau dt_2\sigma_j(t_1)\sigma_j(t_2)\right\rangle\right]\\&=\exp\left[-\tfrac{1}{2}[DP_2(\cos\theta_j)]^2\int_0^{2\tau}(2\tau-t)\sigma_j(0)\sigma_j(2\tau)dt\right].\end{aligned} \tag{15}$$

If the single-particle correlation function

$$g_j(2\tau)=\sigma_j(0)\sigma_j(2\tau)$$

has a simple correlation time τ_c such that

$$g_j(t)\sim\begin{cases}(\bar\sigma_j)^2 & \text{for } t<t_c\\ 0 & \text{for } t>t_c\end{cases}.$$

The above average for the echo amplitude becomes

$$\begin{aligned}E_j(2\tau)&=\exp\{-[\sigma_jDP_2(\cos\theta_j)]^2 2\tau t_c\}\\&=\exp(-\delta_j^2 2\tau t_c).\end{aligned} \tag{16}$$

The echo amplitude is exponentially damped with a relaxation rate $T_2^{-1}=\delta_j^2\tau_c$. $\delta_j=\frac{3}{2}\bar\sigma_jDP_2(\cos\theta_j)$ is just the frequency component of the spectrum contributed by the jth molecule in the slow-motion limit $\omega_m(\simeq 1/\tau_c)\ll D$.

The above results show that the effect of the motion is to remove the spectral components $\Delta\nu=\pm\delta_j$ from the absorption line shape and replace them with a central, motionally narrowed Lorentzian line with a half-width at half-height

$$\Delta\omega_H=T_2^{-1}=\delta_j^2\tau_c. \tag{17}$$

The virtue of studying the echo decays rather than the line shapes lies in the fact that one can distinguish changes in the line shapes due to motional effects from those due to changes in the distribution $P(\sigma)$ of the static order parameters by looking for a motional damping of the solid echoes. This is possible only for fluctuations at frequencies in the range $0.3D\lesssim\omega_m\lesssim 3D$.

The result for the motional damping contains two important results. Firstly, the damping $T_2^{-1}=\delta_j^2\tau_c$ depends on the isochromat studied, even if τ_c is the same for each molecule—components at $\Delta\nu=D$ relax 4 times faster than those at $\Delta\nu=D/2$. As explained earlier, this can lead to a narrow, sharply peaked central component for the motionally averaged spectrum contributed by sites with small σ_j. Furthermore, although the damping of each isochromat is exponential with $T_2^{-1}=\delta_j^2\tau_c$, for this very simple model the variation of T_2 with δ_j will lead to a complex nonexponential damping for the observed echo of the entire sample. These characteristics need to be tested for single crystals in the Pa_3 phase, for which δ_j can be changed in a known fashion by varying the orientation of the magnetic field with respect to the crystal axes. A second feature of the result obtained is that the criterion for the onset of motional damping of the component $\Delta\nu$ of the line shape is given by the condition that

$$0.3\,|\Delta\nu|^2\tau\lesssim\frac{\omega_m}{2\pi}(\simeq\tau_c)\lesssim 3\,|\Delta\nu|^2\tau,$$

τ being the pulse separation. Since practical values of τ are limited by (i) the contribution to the relaxation due to the intermolecular nuclear dipole interactions of strength $d\simeq 1$ kHz, and (ii) the duration of the free induction decay given by $D^{-1}\simeq 30$ μsec; experimental choices of τ are restricted to

$$3D^{-1}(\sim 100\ \mu\text{sec})\lesssim\tau\lesssim d^{-1}(\sim 1\ \text{msec}).$$

For the components $10d < \Delta\nu < D$, motional narrowing will be detectable for

$$100d^2D^{-1}(\sim 1\ \text{kHz}) \lesssim \omega_m \lesssim 0.1D^2d^{-1}(\sim 10^3\ \text{kHz}) . \quad (18)$$

Motion at frequencies lower than those that can be detected by the damping of solid echoes can be observed by studying the attenuation of stimulated echoes produced by a three-pulse sequence. This is discussed in detail in Ref. 15 and we will only give the salient features in this paper. Two rf pulses separated by a time interval τ are used to prepare the system of nuclear spins with a distribution of local nuclear-spin-polarization temperatures β_j (specifying the $\langle I_{Z_j} \rangle$) and local spin-alignment temperatures γ_j (specifying the values $\langle I^2_{Z_j} \rangle$). These values are determined by the mean values of the local order parameters $\bar{\sigma}_j$ during the short time interval τ. Following a waiting period $T_w \gg \tau$, a third pulse is used to convert the "stored" longitudinal components $\langle I_{Z_j} \rangle$ and $\langle I^2_{Z_j} \rangle$ into transverse components such as $\langle I_{X_j} \rangle$ and $\langle I^2_{X_j} \rangle$ which produce a stimulated echo a time τ after the third pulse. This occurs because the evolution during the two time intervals of length τ, before and after the waiting period T_w, are determined by the same Hamiltonian, the secular part of $\mathcal{H}_{DD}^{\text{intra}}$—the evolution occurring during $0 < t < \tau$ is "stored" during $T_w + \tau < t < (T_w + \tau) + \tau$, provided $\mathcal{H}_{DD}^{\text{intra}}$ remains constant. Here we assume that $T_w < T_1$, so that longitudinal relaxation effects can be neglected or unambiguously corrected by independent measurements of T_1. We also neglect attenuation due to spectral diffusion induced by the intermolecular dipolar interactions.

If the order parameters σ_j or the orientation of the symmetry axes [given by (θ_j, ϕ_j)] vary during the waiting period T_w, $\mathcal{H}_{DD}^{\text{intra}}$ will not be the same during the two time intervals τ; the evolution before and after T_w will differ and the echo amplitude will be reduced. This motional damping of the stimulated echo can be used to detect variations of the order parameters during T_w, and the analysis given in Ref. 15 shows that damping can be detected for motion in the range

$$(D^2\tau^2 T_w)^{-1} \lesssim \omega_m^{\text{st}} \lesssim D^2\tau . \quad (19)$$

This extends the frequency range that can be covered by the use of solid echoes by 2—3 orders of magnitude, depending on practical limitations on T_w. In practice, it is limited by spectral diffusion, which for solid hydrogen has limited the lower limit of the observation window to frequencies $\omega_m \gtrsim 100$ Hz. This limit can be lowered once a better quantitative understanding of spectral diffusion has been achieved.

V. LONGITUDINAL NUCLEAR RELAXATION RATES

The decay of the solid echoes and stimulated echoes can be used to probe the spectral density of the molecular fluctuations for frequencies up to $\sim 10^2$—10^3 kHz. Motion at higher frequencies can be explored by measuring the longitudinal nuclear relaxation rates T_1^{-1}. These rates measure the spectral density of the fluctuations at the nuclear Larmor frequency ω_0 and at $2\omega_0$ since it is only the local magnetic field fluctuations at these frequencies that can induce transitions between the nuclear Zeeman levels and thereby restore thermal equilibrium following any perturbation. The fluctuating magnetic fields that drive these transitions arise from the modulation of the intramolecular nuclear dipole-dipole coupling $\mathcal{H}_{DD}^{\text{intra}}$ and the spin-orbit or spin-rotational coupling $\mathcal{H}_{\text{SR}} = C\vec{\mathbf{I}}\cdot\vec{\mathbf{S}}$ by the molecular motion. A straightforward calculation (given in the Appendix) shows that the contributions to the relaxation by $\mathcal{H}_{DD}$ and $\mathcal{H}_{\text{SR}}$ are given by[17,44]

$$(T_1^{-1})_D = \tfrac{9}{16}D^2 \sum_{m=\pm 1,\pm 2} m^2 \mathcal{J}_{2m}(|m|\omega) \quad (20a)$$

and

$$(T_1^{-1})_{\text{SR}} = \tfrac{1}{4}C^2 \sum_{m=\pm 1} |m| \mathcal{J}_{1m}(|m|\omega) , \quad (20b)$$

respectively, where $\mathcal{J}_{2m}(m\omega)$ are the spectral densities given by the Fourier transforms of the autocorrelation functions $\langle \Theta_{2m}(0)\Theta^{\dagger}_{2m}(t) \rangle$. Θ_{2m} are the spherical tensorial operators introduced in Sec. II,

$$\mathcal{J}_{2m}(m\omega) = \int_{-\infty}^{\infty} \langle \Theta_{2m}(t)\Theta^{\dagger}_{2m}(0) \rangle_T e^{im\omega t} dt . \quad (21)$$

The Θ_{1m} are by the operator equivalents of the harmonic functions Y_{1m} in the $J=1$ manifold.

As in the case of the damping of the NMR echoes, it can be shown[17,45] that T_1 depends strongly on the particular isochromat of the line shape studied. The relaxation rate $(T_1^{-1})_{DD}$ is much faster in the center of the line than in the wings, and care must be exercised in analyzing the results. This has been overlooked in some discussions[46] of the value of the T_1 minimum for a powdered sample assuming Lorentzian spectral densities. This dependence on σ_j and the dependence on the orientation (θ_j, ϕ_j) of the local symmetry axes does explain the spectral dependence of T_1 reported by Meyer *et al.*[11,21] and is discussed in the Appendix.

Nuclear-magnetic-resonance experiments on solid hydrogen at low temperature have been carried out for Larmor frequencies $1 \lesssim \omega_0/2\pi \lesssim 300$ MHz, and relaxation studies can therefore be used to probe the orientational fluctuations for frequencies in the $(10^6$—$10^9)$-Hz range. Coupling these experiments with studies of the damping of NMR echoes, we can, in principle, follow the molecular orientational dynamics over the entire frequency domain 10^2—10^9 Hz without any gaps. This would, of course, require the exploitation of a wide variety of NMR techniques for magnetic fields varying from a few hundred gauss to 10 T.

VI. CORRELATION FUNCTIONS AND DEFINITION OF A QUADRUPOLAR GLASS

We have seen in the above sections how the behavior of the autocorrelation functions determines the damping of the NMR spin echoes, motional narrowing of the absorption line shapes, and the longitudinal nuclear-spin-lattice relaxation rates. In order to have a precise formalism as a basis for discussing these phenomena, and to explain unambiguously how information concerning the molecular motion can be extracted from the NMR results, we

considered the simple single-particle correlation function $G_i(t)$ introduced in Sec. II. $\langle\ \rangle_T$ designates a statistical thermodynamic average. We found that, for long times,

$$G_i(\infty)=\sum_m |\langle\Theta_{2m_i}\rangle|^2=q_i^2 ,$$

where $q_i=(\sigma_i^2+\eta_i^2)^{1/2}$ is the magnitude of the total quadrupolarization of the ith molecule, and the parameters σ_i and η_i are to be calculated in the local principal-axes reference frame.

Experimentally, we only study the average

$$\bar{G}(t)=\frac{1}{N}\sum_i G_i(t) ,$$

and the discussion that follows refers to this sample average. For very short times, $t_s \lesssim \hbar/V_{\text{molec}}(\sim 10^{-10}$ sec), $G(t)$ decreases rapidly (see Fig. 3) due to fast fluctuations that occur on a scale determined by the intermolecular potential V_{molec}. It is on this time scale that the libron modes of the Pa_3 structure modulate the molecular orientations at frequencies of ~ 10 GHz. The NMR experiments do not probe these high-frequency modes directly.

The nuclear-spin relaxation studies determine the spectral density of the fluctuations in the frequency range 10^6–10^9 Hz, and thus the behavior of $G(t)$ for $10^{-8}<t<10^{-6}$ sec. In the long-range Pa_3 ordered structure, the main contribution (at temperatures close to T_c) is due to second-order Raman processes involving the absorption and emission of two librons.

The next time interval, $10^{-5}<t<10^{-4}$ sec, in $G(t)$ is covered by cw line-shape studies. As discussed above, the line shapes are determined by the values of the "quasistatic" order parameters $\bar{\sigma}_j$ and $\bar{\eta}_j$ determined over the frequency interval $0.1D<\omega_m<D$, where $D\sim 10^5$ Hz in the strength of the intramolecular dipolar interaction. Changes in the behavior, e.g., changes in the slope of $G(t)$ as one alters the temperature, in this time interval will lead to changes in the line shapes. The value of $G(t)$ for $0.1D^{-1}<t<10D^{-1}$ determines the intramolecular contribution to the NMR second moment M_2, *provided* that $G(t)$ varies only very slowly in the interval $0.1D^{-1}<t<10D^{-1}$. In this case, $M_2^{\text{intra}}=D^2G(D^{-1})$. The hypothesis that one can interpret the line shape in terms of a superposition of Pake doublets (using a distribution of order parameters, if necessary) is based on the assumption that $G(t)$ is almost perfectly flat in the region $0.1d^{-1}<t<10D^{-1}$; if this is not true, the NMR line shape can be motionally narrowed as explained earlier.

The distinction between motional-narrowing effects and simple changes in the distribution of the quasistatic order parameters can be made by studying the damping of solid echoes. As explained in Sec. IV, these pulsed NMR studies explore the t dependence of $G(t)$ for $10^{-5}<t<10^{-3}$ sec, since the echoes are subject to an additional motional damping (i.e., in addition to those due to the static intermolecular nuclear spin-spin interactions) for orientational fluctuations in the range $(10d)^2D^{-1}\lesssim\omega_m\lesssim(0.1D)^2d^{-1}$, where d is the strength of the intermolecular dipole interactions.

In order to probe $G(t)$ for longer times, studies of the attenuation of stimulated echoes are carried out. As seen above, these echoes are motionally damped for molecular motion in the range $(d^2\tau^2T_1)^{-1}\lesssim\omega_m\lesssim D^2\tau$ with $\tau_{\min}\sim 3D^{-1}$ and $\tau_{\max}\sim 3d^{-1}$. These recently developed techniques[15,18,10] therefore extend our observational time window for studies of $G(t)$ to the upper limit $t_{\max}^{\text{st}}\simeq(4\pi^2D^2\tau^2)T_1$, which can be of the order of 10^2 sec. This is shown in Fig. 3. As a result of the spectral diffusion and the absence of a reliable theoretical treatment of its effect, $t_{\max}$ is limited not by T_1, as given in the above formula, but by this diffusion, and published experimental studies have been limited to $t_{\max}^{\text{st}}\sim 0.1$ sec.[15]

The aim of the NMR experiments discussed in Ref. 15 was to look for molecular motion in the "ultralow"-frequency interval $10^{-2}<\omega_m<10^4$ Hz. At high temperatures, in the completely disordered phase, the molecular orientations fluctuate rapidly with $\omega_m\sim\hbar^{-1}V_{QQ}$, and since $\omega_m\gg 0.1D^2d\sim 10^3$ kHz, the motion is too fast to affect the stimulated echoes. If the characteristic molecular motion does slow down to frequencies $\omega_m<10^2$ kHz, an additional motional damping can be seen as soon as ω_m falls in the observational "window"

$$(D^2T_1)^{-1}10d^2\lesssim\omega_m^{\text{st}}\lesssim 0.1D^2d(\sim 10^3\text{ kHz})$$

given by Eq. (17) for $\tau\lesssim 0.1d^{-1}\simeq 0.1$ msec. In practice, τ is chosen in the interval $0.03\lesssim\tau\lesssim 3$ msec; the lower limit avoids excessive interference with the free-induction-decay transients after the third pulse, while the upper limit is imposed by the effects of spectral diffusion. Note that this upper limit for ω_m^{st} (for which the stimulated echoes are modified) can, by a suitable choice of τ, overlap the interval for which motional narrowing of the line shapes can occur.

Observation of the motional damping of the stimulated

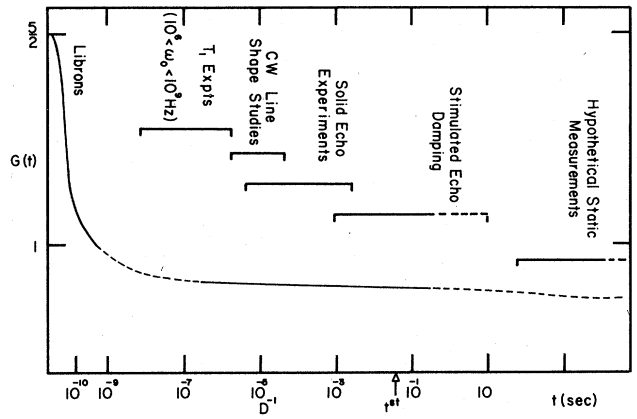

FIG. 3. Variation of the autocorrelation function $G_j(t)=\frac{1}{2}\langle\Theta_{2m_j}(t)\Theta_{2m_j}^{\dagger}(0)+\Theta_{2m_j}(0)\Theta_{2m_j}^{\dagger}(t)\rangle_T$ as a function of time t for different time scales that can be probed by various NMR techniques. There is a rapid drop from $G_j(0)=\frac{5}{2}$ for small times t_{micro} determined by the microscopic interactions V_{molec}. The limit $G_j(\infty)$ gives the equilibrium value of the square quadrupolarization $q_j^2=\sigma_j^2+\eta_j^2$. If $G_j(t)$ is flat from t_{micro} to t_{xx}, the molecular orientations are said to be "frozen" on that time scale. In addition, if it can be established that $G(t_{xx})>q_{\text{eqm}}^2$ (by independent experiments), then the basic criteria for a quadrupolar glass have been satisfied.

echoes remains possible as long as there is significant motion in the spectral window

$$(D^2\tau^2 T_w)^{-1} \leq \omega_m \leq D^2\tau \,, \tag{22}$$

and different intervals of the time scale for $G(t)$ can be explored by selecting different values of τ and T_w in the $90°$-τ-θ-T_w-θ-τ sequence. For a given sample one then expects to observe a supplementary damping of the stimulated echo for those temperatures for which condition (22) is satisfied. At lower temperatures no such motional damping would be observed. Some experimental evidence was reported for such effects in Ref. 15. A (30%) damping (after correction for T_1 effects) was observed in the temperature interval $240 < T < 270$ mK for a solid hydrogen sample ($x_{\text{ortho}} = 38$ at. %). The experimental conditions were $\tau = 25$ μsec and $T_w = 2$ msec, for which $80 \leq \omega_m^{\text{st}} \leq 2.5 \times 10^5$ Hz.

This effect was not seen in studies carried out elsewhere[18] for bulk samples for which temperature differentials were believed to be less than 10 mK across the sample for concentrations $x \sim 38$ at. %.[47] Only the *average* temperature was known for the experiments described in Ref. 18, but the quoted temperature inhomogeneities would appear to be too small to wash out the effect. As explained above in detail, there is an intrinsic inhomogeneity in the samples since the relevant frequency scale for damping depends on $P_2(\cos\theta_i)$ *even* if the motion of each molecule is the same. This, and the fact that different molecular clusters in the dilute sample can be expected to fluctuate at different rates, leads to a strong inhomogeneity for the motional damping. This means that the weak damping observed for $250 < T < 270$ mK can be understood as a sum of effects from different regions of the sample. For the purposes of illustration we consider a specific example. If, upon cooling, the motion of all molecules slows down to $10^2 < \omega_m < 10^5$ Hz, in a very narrow temperature interval $250 < T < 255$ mK, the above inhomogeneity effect which leads to motional damping when

$$\omega_m(i) = \omega_m P_2(\cos\theta_i)$$

falls in the interval 10^2–10^5 Hz, *will* lead to a weak damping observed throughout the wider temperature interval 240–270 mK. The absence of any significant modification of the stimulated echoes (apart from T_1 effects) for this pulse sequence below 240 mK is taken as evidence that there is no significant motion occurring for frequencies $\omega_m > 80$ Hz at $T < 240$ mK. This means that, within experimental error, $G(t)$ is essentially flat for $D^{-1} < t < \frac{1}{80}$ sec. We can now say that the molecular orientations appear to be "*frozen*" for this time scale.

Returning now to the general terms that have been used to discuss the molecular ordering in solid hydrogen mixtures, a rigorous definition of the term "frozen molecular orientations" for a specified time scale t_{scale} is now given by the following:

(i) $G(t)$ is flat over the time scale $D^{-1} < t < t_{\text{scale}} + D^{-1}$;

(ii) $G(t_{\text{scale}}) > q_{\text{eqm}}$, where q^2_{eqm} is the statistical average of q^2 obtained by taking into account *all* possible configurations.

The statistical average q^2_{eqm} is represented by the foot $G(\infty)$ of Fig. 3 at $t = \infty$. [The condition $t > D^{-1}$ in (i) is to avoid the case of motional-narrowing effects for the line shapes.] These two rigorous criteria define the term "glass" or "glassy state" (or, in our case, "quadrupolar glass") that has been used rather loosely to describe the NMR results for those solid ortho-para hydrogen mixtures for which no long-range periodic order has been detected. The first condition is satisfied by the stimulated-echo experiments for $t_{\text{scale}} \sim 10^{-2}$ sec, but the NMR results alone are unable to prove the second criterion.

The underlying physics of the second condition is that some aspect of nonergodic behavior is present. More precisely, we mean that for experimental time scales extending up to t_{scale} not only has no evolution been detected, but furthermore the system has not attained thermal equilibrium, i.e.,

$$q^2_{\text{expt}} \neq q^2_{\text{eqm}} \,.$$

Careful thermodynamic measurements coupled with studies of transport properties as well as NMR experiments may help test this condition. In view of the possible absence of thermal equilibrium, the system is referred to as a "glassy state" rather than a "glass phase."

In view of the absence of any sign of a sudden "transition" (as stressed originally by Schweizer *et al.*[48]) from the para-orientational phase to a "glass" state satisfying the above conditions (which is seen for the magnetic dipolar glasses[34]), the results are often[45] interpreted in terms of a "dynamic gel" in which the characteristic spectral density shifts to lower-frequency ranges very rapidly as the temperature is reduced (with an explicit T dependence of a cooperative effect for the mutual slowing down of the molecular reorientations) until the observational window provided by the particular window is exceeded. A "dynamic gel" is then described by conditions (i) and (ii) above, with the feature that the origin of the evolution is

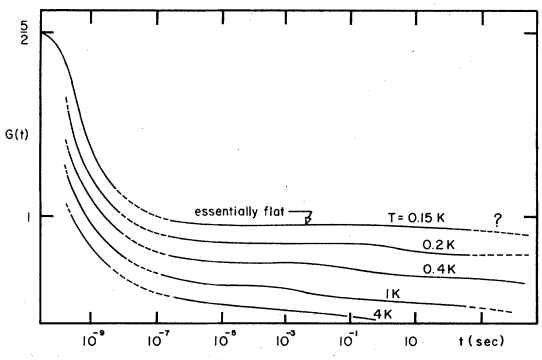

FIG. 4. Example of a possible evolution of $G(t)$ with temperature consistent with NMR measurements. The behavior beyond $t = 10^{-2}$ sec is unknown, and the discrepancies in the T_1 data of different groups leave the region $10^{-7} < 10^{-5}$ sec undetermined. It is important to realize that the question of glass formation is determined by (i) the flatness of $G(t)$ for $10^{-5} < t < t_{\text{max}} \simeq 10^{-2}$ sec, and (ii) the difference between $G(t_{\text{max}})$ and $G(\infty)$.

in the temperature dependence of the molecular dynamics. A schematic representation showing the evolution of $G(t)$ as the temperature is lowered in given in Fig. 4 for the case of a smooth dynamic gel.

One fact is clear, namely that all the available NMR results are consistent with condition (i) and no experiments of any kind have disproved condition (ii). Evidence against quadrupolar glass formation (according to the criteria and definitions given here) has not been found.

VII. CONCLUSION

We have presented here a definition of the orientational-order parameters for ortho hydrogen molecules in solid-hydrogen mixtures. These parameters are, in turn, used to write generalized single-particle autocorrelation functions which determine the results of various NMR experiments.

This formalism is used to provide unambiguous definitions of terms such as "freezing," "dynamic gel," and "quadrupolar glass formation," which have been used to discuss and interpret the NMR results. It is shown that two conditions must be met in order to claim the existence of a quadrupolar glass as we have defined it. The NMR results obtained by most groups are certainly consistent with these conditions. While the first condition seems established, the second condition related to the lack of ergodicity (whether it be due to a "transition" to a glass regime or a "slowing down" of the molecular dynamics) needs to be tested by further experiments sensitive to the thermodynamic properties of these systems.

ACKNOWLEDGMENTS

Numerous discussions with D. G. Haase, A. B. Harris, J. R. Gaines, M. A. Klenin, H. Meyer, and R. V. Pound are gratefully acknowledged. This work and one of us (N.S.S.) were supported in part by National Science Foundation Low Temperature Physics Program Grant No. DMR-83-04322.

APPENDIX: LONGITUDINAL NUCLEAR-SPIN LATTICE RELAXATION

The total Hamiltonian $\mathscr{H}_T$ governing the rate at which the nuclear spins of ortho molecules come into thermal equilibrium is given by the sum of three Hamiltonians:

$$\mathscr{H}_T=\mathscr{H}_Z+\mathscr{H}_M+\mathscr{H}_C \ . \tag{A1}$$

The Zeeman Hamiltonian

$$\mathscr{H}_Z=\sum_i \hbar\omega_0 I_{iz} \tag{A2}$$

describes the energy levels of noninteracting nuclear spins is an external magnetic field B_0 ($\omega_0=\gamma B_0$). The index i labels a given molecule. The molecular Hamiltonian

$$\mathscr{H}_M=\tfrac{1}{2}\sum_{i,j}\sum_{m,n}(\Gamma_{ij})_{mn}\Theta_{2m}(i)\Theta_{2n}(j) \tag{A3}$$

describes the electrostatic quadrupole-quadrupole interaction between the molecules, and determines the quadrupolar degrees of freedom of the molecules in the interaction. The Θ_{2m} are the irreducible tensorial operators defined in Sec. II and $(\Gamma_{ij})_{mn}$ is the mnth component of the quadrupole-quadrupole coupling between the ith and jth molecules.[39,17] The coupling between the nuclear spins and the orientational degrees of freedom which provides the mechanism for achieving thermal relaxation is given by the intramolecular nuclear dipole-dipole interactions $\mathscr{H}_{DD}$ and the spin-rotational coupling $\mathscr{H}_{SR}$ of each molecule,

$$\mathscr{H}_C=\mathscr{H}_{DD}+\mathscr{H}_{SR} \ , \tag{A4a}$$

$$\mathscr{H}_{DD}=h\sum_i D\sum_m T^{\dagger}_{2m}(i)\mathscr{H}_{2m}(i) \ , \tag{A4b}$$

and

$$\mathscr{H}_C=-h\sum_i C\vec{\mathrm{I}}_i\cdot\vec{\mathrm{J}}_i \ . \tag{A4c}$$

The T_{2m} are irreducible tensorial operators for the nuclear-spin degrees of freedom in the manifold $I=1$ analogous to the operators Θ_{2m} for the orientational degrees of freedom,

$$T_{20}=1-\tfrac{3}{2}I_Z^2 \ ,$$

$$T_{2,\pm1}=\pm(\tfrac{3}{8})^{1/2}(I_{\pm}I_Z+I_ZI_{\pm}) \ ,$$

and

$$T_{2,\pm2}=(\tfrac{3}{8})^{1/2}(I_{\pm})^2 \ .$$

$$D/2\pi=173.1 \text{ kHz and } C/2\pi=114 \text{ kHz} \ .$$

As a result of the coupling $\mathscr{H}_C$, each nuclear spin experiences local fluctuating magnetic field, and it is the components of these fluctuations at the Larmor frequency ω_0 and at $2\omega_0$ that induce transitions between the nuclear-spin levels and thereby assure thermal equilibrium.

In the limit in which the nuclear spins can be considered as only very weakly coupled, the longitudinal relaxation rate of each molecule i can be written as an integral of the local spin-torque correlation $K(t)$,[49]

$$T_{1i}^{-1}=\int_0^{\infty}K_i(t)dt \ , \tag{A5}$$

where

$$K_i(t)=\langle[I_{iZ},\mathscr{H}_C](t)[I_{iZ},\mathscr{H}_C]^{\dagger}(0)\rangle_T \ . \tag{A6}$$

The time dependence indicated for the operators is given by the interaction representation $A(t)=e^{i\mathscr{H}_0 t}A\,e^{-i\mathscr{H}_0 t}$ with $\mathscr{H}_0=\mathscr{H}_Z+\mathscr{H}_M$. [This form for $K(t)$ is only valid for times $t>h/k_BT$.]

After evaluating the commutators in Eq. (A6) and calculating the thermal averages $\langle\ \rangle_T$, we find

$$T_{1_i}^{-1}=T_{1D}^{-1}+T_{1C}^{-1} \ , \tag{A7a}$$

where

$$T_{1D}^{-1}=\tfrac{1}{2}D^2\int_0^{\infty}dt\sum_{m=-2}^{2}m^2\langle\Theta_{2m}(t)\Theta^{\dagger}_{2m}(0)\rangle_T e^{im\omega_0 t} \tag{A7b}$$

and

$$T_{1C}^{-1}=\tfrac{1}{2}C^2\int_0^\infty dt\sum_{m=-1}^{1}m^2\langle J_m(t)J_m^\dagger(0)\rangle_T e^{im\omega_0 t}\,. \tag{A7c}$$

(The site index i has been dropped where no confusion arises.) These results can be written in terms of the spectral densities of the correlation functions,

$$\mathcal{J}_{2m}(\omega)=\int_{-\infty}^{\infty}dt\langle\Theta_{2m}(t)\Theta_{2m}^\dagger(0)\rangle_T e^{i\omega t} \tag{A8a}$$

and

$$\mathcal{J}_{1m}(\omega)=\int_{-\infty}^{\infty}dt\langle J_m(t)J_m^\dagger(0)\rangle_T e^{i\omega t}\,. \tag{A8b}$$

This gives the compact form

$$T_1^{-1}=\tfrac{1}{2}D^2[\mathcal{J}_{21}(\omega_0)+4\mathcal{J}_{22}(2\omega_0)]+\tfrac{1}{2}C^2\mathcal{J}_{11}(\omega_0)\,. \tag{A9}$$

In the Pa_3 phase for high ortho concentrations the spectral densities can be evaluated in a straightforward fashion since the fundamental excitations (librons or librational waves) and their densities of states are well understood.[44,50] The dominant contribution to the spectral densities is given by the Raman scattering of the librons by the nuclear spins. The result[49] is

$$T_{1i}^{-1}=[(\tfrac{1}{6}C^2+\tfrac{5}{8}D^2)-(\tfrac{1}{6}C^2+\tfrac{1}{8}D^2)P_2(\cos\gamma_i)]I\,, \tag{A10a}$$

where γ_i is the angle between the applied magnetic field B_0 and the equilibrium orientation of the ith molecule. We have

$$I=\int dE\,\rho^2(E)\eta(E)\,, \tag{A10b}$$

where $\rho(E)$ is the libron density of states and $\eta(E)=[\exp(\beta E)-1]^{-1}$ is the boson population factor.[51]

The result given by Eqs. (A10) shows that the relaxation time is spatially inhomogeneous as a result of the factor $P_2(\cos\gamma_i)$, which varies from one sublattice to another, and also depends on the orientation of the individual crystals in the sample relative to the applied magnetic field. This variation is also that which determines the spread of frequencies in the absorption spectrum. (The order parameter σ has the same value at each site in the Pa_3 structure.) The value of T_1 therefore depends on the particular isochromat of the spectrum. This inhomogeneity has not been observed experimentally and we believe that this is due to a rapid homogenization of the nuclear-spin temperatures in the Pa_3 phase. The rapid homogenization or spectral diffusion is affected by the flip-flop terms in the intermolecular nuclear dipole-dipole interactions between different molecules.

In the quadrupolar glass phase we do not know the nature of the excitations and we cannot proceed with the calculation of the spectral densities. Care is needed in even formulating the relaxation rates since (i) the observation of an overall quadrupolarization at low temperature shows that the correlation functions defined in Secs. II and VI are nonzero in the limit $t\to\infty$, and (ii) the local principal axes vary from site to site. In order to attempt to evaluate the overall behavior of T_1, we will hypothesize that we can separate the behavior at long times from that for short times and further that it is the fluctuations for short times that determine T_1. We therefore assume that the limit

$$\lim_{t\to\infty}\langle\Theta_{2m}(t)\Theta_{2m}^\dagger(0)\rangle_T=\langle\Theta_{2m}\rangle_T^2$$

exists, which implies that the orientations are partially frozen. In this case the relaxation is determined by the fluctuations

$$\langle\Theta_{2m}\rangle_T-\langle\Theta_{2m}\rangle_T^2 \quad\text{and}\quad \langle J_m^2\rangle_T-\langle J_m\rangle_T^2\,.$$

The calculation of the spectral densities is carried out in the local reference frame for each molecule (given by the principal axes for the quadrupolarization). The relaxation rate for each molecule is found to be given by

$$T_1^{-1}=T_{1DD}^{-1}+T_{1SR}^{-1}\,,$$

where

$$T_{1DD}^{-1}=\frac{D^2}{12}\begin{bmatrix}(1-\sigma)(1+2\sigma)[\frac{2}{3}(1+y-2y^2)j_{20}(\omega_0)+\frac{4}{3}(1-2y+y^2)j_{20}(2\omega_0)]\\(1+\sigma/2)[\frac{2}{9}(2-y+8y^2)j_{21}(\omega_0)+\frac{4}{9}(8-4y+4y^2)j_{21}(2\omega_0)]\\(1-\sigma)[\frac{4}{9}(2-y+y^2)j_{22}(\omega_0)+\frac{4}{9}(7+10y+y^2)j_{20}(2\omega_0)]\end{bmatrix} \tag{A11a}$$

and

$$T_{1SR}^{-1}=\frac{C^2}{9}[(1-\sigma)(1+2y)j_{10}(\omega_0)+2(2+\sigma)(1-y)j_{11}(\omega_0)]\,. \tag{A11b}$$

σ is the local quadrupolarization which is assumed to be axial, and $y_i=(1/\sigma_i)P_2(\cos\gamma_i)$, where γ_i is the angle between the local symmetry axis of the ith molecule and the applied field. The normalized spectral densities

$$j_{2m}(\omega)=\frac{\int_{-\infty}^{\infty}dt\,e^{i\omega t}\langle\theta_{2m}(t)\theta_{2m}^\dagger(0)\rangle_T}{\langle\Theta_{2m}(0)\Theta_{2m}^\dagger(0)\rangle_T}\,, \tag{A12}$$

where

$$\theta_{2m}+\Theta_{2m}-\langle\Theta_{2m}\rangle\,.$$

The importance of the above result is that even if we assume that the local dynamics is uniform from site to site, the nuclear relaxation rates are nevertheless *inhomogeneous*. This inhomogeneity is due to two factors: (i) the distribution of the angles γ_i due to the different orientations of the local symmetry axes, and (ii) the variation of the quadrupolarizations from one site to another. While the

authors of Ref. 21 did offer an explanation for the variation of T_1 with $\Delta\nu$, the results obtained here are more general.

These results can be used to explain recent observations of the spectral inhomogeneity by Washburn *et al.*[11,21] These authors found that the relaxation time depended strongly on the position of the line in the absorption spectrum with the wings of the line shapes relaxing very slowly compared to the center of the spectrum. This behavior is described by our result given in Eqs. (A11), for which the factor $1-x \to 0$ in the wings of the line.

---

*Permanent address: Service de Physique du Solide et de Résonance Magnétique, Centre d'Etudes Nucléaires de Saclay, F-91191 Gif-sur-Yvette, France.

[1]N. S. Sullivan and R. V. Pound, Phys. Lett. **39A**, 23 (1972); Phys. Rev. A **6**, 1102 (1972).
[2]H. Ishimoto, K. Nagamine, and Y. Kumura, J. Phys. Soc. Jpn. **35**, 300 (1973); **40**, 312 (1976).
[3]N. S. Sullivan, H. Vinegar, and R. V. Pound, Phys. Rev. B **12**, 2596 (1975).
[4]N. S. Sullivan, J. Phys. (Paris) Lett. **37**, L209 (1976); J. Phys. **37**, 981 (1976).
[5]H. J. Vinegar, J. J. Byleckie, and R. V. Pound, Phys. Rev. B **16**, 3016 (1977).
[6]N. S. Sullivan, M. Devoret, B. P. Cowan, and C. Urbina, Phys. Rev. B **17**, 5016 (1978).
[7]N. S. Sullivan and M. Devoret, J. Phys. (Paris) Colloq. **39**, C6-92 (1978).
[8]N. S. Sullivan, M. Devoret, and J. M. Vaissiere, J. Phys. (Paris) Lett. **40**, L559 (1979).
[9]W. T. Cochran, J. R. Gaines, R. P. McCall, P. E. Sokol, and B. R. Patton, Phys. Rev. Lett. **45**, 1576 (1980).
[10]I. Yu, S. Washburn, and H. Meyer, Solid State Commun. **40**, 693 (1981); J. Low Temp. Phys. **51**, 369 (1983).
[11]S. Washburn, I. Yu, and H. Meyer, Phys. Rev. **85A**, 365 (1981).
[12]N. S. Sullivan and D. Estève, Physica **107B**, 189 (1981).
[13]D. Candela, S. Buchman, W. T. Vetterling, and R. V. Pound, Physica **107B**, 187 (1981).
[14]D. Estève and N. S. Sullivan, J. Phys. C **15**, 4881 (1982).
[15]N. S. Sullivan, D. Estève, and M. Devoret, J. Phys. C **15**, 4895 (1982).
[16]S. Washburn, M. Calkins, H. Meyer, and A. B. Harris, J. Low Temp. Phys. **49**, 101 (1982).
[17]M. Devoret, thesis, Université de Paris—Sud, 1982.
[18]I. Yu, S. Washburn, M. Calkins, and H. Meyer, J. Low Temp. Phys. **51**, 401 (1983).
[19]M. Devoret, D. Estève, and N. S. Sullivan, J. Phys. C **15**, 5455 (1982).
[20]A. B. Harris, S. Washburn, and H. Meyer, J. Low Temp. Phys. **50**, 151 (1983).
[21]S. Washburn, M. Calkins, H. Meyer, and A. B. Harris, J. Low Temp. Phys. **53**, 585 (1983).
[22]D. G. Haase, R. A. Orban, and J. O. Sears, Solid State Commun. **32**, 1333 (1979); D. G. Haase, J. O. Sears, and R. A. Orban, *ibid.* **35**, 891 (1980).
[23]D. G. Haase, and A. M. Saleh, Physica **107B**, 191 (1981).
[24]D. G. Haase, Solid State Commun. **44**, 469 (1982).
[25]M. A. Klenin, Phys. Rev. Lett. **42**, 1549 (1979).
[26]M. A. Klenin and S. F. Pate, Physica **107B**, 185 (1981).
[27]D. G. Haase and M. A. Klenin (unpublished).
[28]J. V. Gates, P. R. Ganfors, B. A. Fraass, and R. O. Simmons, Phys. Rev. B **19**, 3667 (1979).
[29]D. Candela and W. T. Vetterling, Phys. Rev. B **25**, 6655 (1982).
[30]P. Candela, S. Buchman, W. T. Vetterling, and R. V. Pound, Phys. Rev. B **27**, 3084 (1983).
[31]D. Candela, Ph.D. thesis, Harvard University, 1983.
[32]V. Canella and J. A. Mydosh, Phys. Rev. B **6**, 4220 (1972).
[33]K. Adkins and N. Rivier, J. Phys. (Paris) Colloq. **35**, C4 (1974).
[34]N. Bontemps, J. Rajchenbach, and R. Orbach, J. Phys. (Paris) Lett. **44**, L47 (1983).
[35]K. H. Michel and J. M. Rowe, Phys. Rev. B **22**, 1417 (1980).
[36]C. W. Garland, J. Z. Kwiecien, and J. C. Damien, Phys. Rev. B **25**, 5818 (1982).
[37]A. Loidl, R. Feile, and K. Knorr, Phys. Rev. Lett. **48**, 1263 (1982).
[38]F. Borsa, U. T. Höchli, J. J. van der Klink, and D. Rytz, Phys. Rev. Lett. **45**, 1884 (1980).
[39]For a review of the properties of solid hydrogen, see I. F. Silvera, Rev. Mod. Phys. **52**, 393 (1980).
[40]V. B. Kokshenev, Solid State Commun. **44**, 1593 (1982).
[41]N. S. Sullivan, in *Quantum Fluids and Solids, 1983,* proceedings of the Third Sanibel Symposium on Quantum Fluids and Solids, Sanibel Island, Florida, 1983, edited by E. D. Adams and G. G. Ihas (AIP, New York, 1983).
[42]J. R. Gaines, A. Mukherjee, and Y. C. Shi, Phys. Rev. B **17**, 4188 (1978).
[43]L. I. Amstutz, H. Meyer, S. M. Myers, and D. C. Rorer, Phys. Rev. **181**, 589 (1969).
[44]A. B. Harris, Phys. Rev. B **2**, 3495 (1970).
[45]Also see contributions by J. R. Gaines, R. V. Pound, and N. S. Sullivan in Ref. 41.
[46]M. S. Conradi, Phys. Rev. B **28**, 2848 (1983).
[47]H. Meyer (private communication).
[48]R. Schweizer, S. Washburn, and H. Meyer, Solid State Commun. **35**, 623 (1980).
[49]A. Landesman, Ann. Phys. (Paris) **8**, 1 (1973).
[50]W. N. Hardy and A. J. Berlinsky, Phys. Rev. B **8**, 4996 (1973).
[51]S. Washburn, I. Yu, and H. Meyer, J. Low Temp. Phys. **53**, 585 (1983).